

Author version: *Geophys. Res. Lett.*, vol.42(4); 2015; 1105–1112

## **Magma production rate along the Ninetyeast Ridge and its relationship to Indian plate motion and Kerguelen hot spot activity**

K.M. Sreejith<sup>1\*</sup>, K.S. Krishna<sup>2</sup>

<sup>1</sup>Geosciences Division, Geosciences and Applications Group, Space Applications Center (ISRO), Ahmedabad, India - 380015

<sup>2</sup>CSIR - National Institute of Oceanography, Dona Paula, Goa, India – 403004

\* Corresponding Author's E-mail: [sreejith81@gmail.com](mailto:sreejith81@gmail.com)

### **Abstract**

The Ninetyeast Ridge (NER), a linear trace of the Kerguelen hot spot in the Indian Ocean, was emplaced on a rapidly drifting Indian plate. Magma production rates along the ridge track are computed using gravity-derived excess crustal thickness data. The production rates change between 2 and 15 m<sup>3</sup>/s over timescales of 3-16 Myr. Major variations in magma production rates are primarily associated with significant changes in the Indian plate velocity with low production phases linked to high plate velocity periods. The lowest magma production rate (2m<sup>3</sup>/s) at 62 Ma is associated with the rapid northward drift of Indian plate under the influence of the Reunion mantle plume. The contemporaneous slowing of the African plate coincides with increase in magma production rate along the Walvis Ridge in the Atlantic Ocean. The present study suggests that variations in the Indian plate motion and frequent ridge jumps have a major role in controlling the magma production, particularly on long period cycles (~16 Myr). Short-period variations (~5 Myr) in magma productions may be associated with intrinsic changes in the plume, possibly due to the presence of solitary waves in the plume conduit.

**Keywords:** Ninetyeast Ridge, Kerguelen hot spot, Magma production, Indian plate motion, Ridge jumps

## 1. Introduction and Tectonic Setting

The Ninetyeast Ridge (NER) extends for more than 5000 km roughly along the 90°E meridian between 30°S and 17°N latitudes in the eastern Indian Ocean (Figure 1). The NER structure has complex morphology, consists of continuous volcanic construct in the south (up to 11°S), relatively shallow discontinuous volcanic highs in the centre (between 11°S and 1°N) and series of large volcanoes northwards to 10°N, while in the Bay of Bengal region the ridge is completely buried under thick Bengal Fan sediments [Curry *et al.*, 1982; Gopala Rao *et al.*, 1997]. Geophysical, geochemical and geochronological data from the NER established that the ridge originated from the Kerguelen hot spot, when the volcanic source was located largely beneath the northward-moving Indian plate from the Late Cretaceous to the Early Cenozoic period [Duncan, 1991; Royer *et al.*, 1991; Krishna *et al.*, 1999; Pringle *et al.*, 2008; Krishna *et al.*, 2012]. The ridge is also unique because it is seismically active and is associated with the Indian Ocean's diffuse deformation zone, acting as a plate boundary between three sub-plates, Indian, Australian and Capricorn [Royer and Gordon, 1997; Gordon *et al.*, 1998; Krishna *et al.*, 2001, 2009; Sager *et al.*, 2013]. New geochronology data from core samples from the Deep Sea Drilling Project (DSDP) Sites 216, 214, 254, and Ocean Drilling Program (ODP) Sites 758, 756 along the NER suggest a linear age progression from north (77 Ma at ODP Site 758) to south (43 Ma at DSDP Site 254), suggesting an emplacement rate of about 118 km/Myr [Pringle *et al.*, 2008]. However, the rate of accretion of adjacent ocean basin based on the magnetic data is about half (48–58 km/Myr) that of the NER [Krishna *et al.*, 2012], suggesting southward jumps of the Wharton spreading ridge segments leading to transfer of parts of oceanic crust from the Antarctic plate to the Indian plate [Royer *et al.*, 1991; Krishna *et al.*, 1999; Krishna *et al.*, 2012].

Magma production rate along the hot spot track is important for understanding the spatial and temporal behavior of mantle plumes, hot spot-spreading ridge interactions and variations in plume conduits [Mjelde *et al.*, 2010 and references therein]. Variations in magma production rates along major hot spot tracks, such as Reunion, Hawaiian, Louisville and Walvis have been investigated by several workers [White, 1993; Vidal and Bonneville, 2004; Van Ark and Lin, 2004, Tiwari *et al.*, 2007]. Coffin *et al.*, [2002] estimated the average eruption rates of the Kerguelen Plateau, Broken Ridge, Ninetyeast Ridge and associated Cretaceous magmatism found near the continental margins of India, Australia and Antarctica and provided a rough estimation of 0.1 km<sup>3</sup>/yr (3.2 m<sup>3</sup>/s) magma flux for the entire NER track. However, detailed study of the magma production rates along the Kerguelen hot spot trace, particularly along the NER has not been carried out previously. In this study, for the first time, we

estimated the variations in magma production rates along the NER from 43 Ma to 77 Ma. These variations are related to changes in velocity of the northward moving Indian plate and jumps of the Wharton Basin spreading centre towards the Kerguelen hot spot.

## **2. Geophysical Data**

We have utilized satellite derived bathymetry [*Smith and Sandwell, 1997*], free-air gravity [*Sandwell and Smith, 2009*], sediment thickness [*Levchenko et al., 1993; Curray, 1994; Divins, 2001*] and seafloor age [*Müller et al., 2008*] data from the NER and adjacent oceanic basins. Then we computed the Residual Mantle Bouguer Anomaly (RMBA) data for the NER using free-air gravity anomaly data and inverted to generate a crustal thickness map [for computational details refer *Sreejith and Krishna, 2013*]. The derived crustal thickness data are, in turn, used for the calculation of magma production rates along the ridge track and utilized for understanding the spatial and temporal behavior of the Kerguelen hot spot and its possible relationship with Indian plate motion.

## **3. Computation of Magma Flux along the NER**

Magma production rates along the hot spot tracks are usually computed assuming Airy or flexural isostatic compensation mechanisms for the volcanic loads [*White, 1993; Tiwari et al., 2007*]. In general, the choice of isostatic compensation mechanism does not have a significant influence on the final results, as the computed volcanic volumes are unchanged [*Vidal and Bonneville, 2004*]. In an alternative approach, *Van Ark and Lin [2004]* utilized crustal thickness data for computation of magma volume flux along the Hawaiian hot spot track. As the NER track possess highly segmented isostatic compensation ( $T_e=4-35$  km) together with underplated volcanic material beneath the crust [*Sreejith and Krishna, 2013*], we used RMBA derived crustal thickness data of the ridge including the underplated rocks, for the magma volume computations. A reference crustal thickness of 6 km was subtracted from the crustal thickness data of the NER and the excess crustal thickness was calculated. Further we used the method of translating windows along the hot spot track [*Vidal and Bonneville, 2004*] for the magma volume computations. The volume of extra crust ( $\Delta V$ ) is computed along a window, and then the window is systematically moved along the axis of the NER from latitudes 28°S to 8°N. A series of computations were done to choose the optimum window size for the volume flux estimation. Windows with width of 550 km and length 110 km is found to be optimum to capture the maximum width of NER (about 500 km) and along axis variations in the crustal thickness respectively. The volume flux is computed by dividing  $\Delta V$  by the difference in age of the ridge between the northern and southern ends of each

window ( $\Delta T$ ) as derived from a linear interpolation of the new geochronology data of core samples from the DSDP Sites 216, 214, 254 and ODP Sites 758, 756 along the NER [Pringle *et al.*, 2008].

Magma production rates are found to be highly variable ranging from 2 to 15 m<sup>3</sup>/s along the NER track (Figure 2a). Our results agree with an earlier estimate of an average 0.1 km<sup>3</sup>/yr (3.2 m<sup>3</sup>/s) magma flux for the NER [Coffin *et al.*, 2002]. However, the overall magma production rates are higher in our case due to the methodology adopted. Coffin *et al.* [2002] have followed a simple procedure of considering the total volume of NER estimated by Grevemeyer *et al.* [2001] and divided it by age difference of the ridge from north to south (from 85 to 35Ma). In the present study we have computed the volume flux using crustal thickness data of the ridge [Sreejith and Krishna, 2013]. An important observation in our result is the extremely low magma production of about 2m<sup>3</sup>/s at ~62 Ma, flanked by high production rates of about 12 m<sup>3</sup>/s and 15 m<sup>3</sup>/s.

Power Spectral Density (PSD) was calculated to quantify the temporal variations in magma production rates along the NER (Figure 3). The spectral energy has significant peaks at 16.5 and 5.5 Myr which are interpreted to reflect long and short period oscillations in magma production along the ridge track. The period 16.5 Myr appears to indicate average long period variations between the peaks at 53, 57.5, 70.6 and 73.6 Ma, whereas the period 5.5 Myr may reflect the short term variations in the magma flux plot with various peaks/troughs spaced between 2.9 – 6.6 Myr (Figure 3).

#### **4. Magma production rate and its relationship with the Indian plate motion**

The NER track possesses a variable magma production rates ranging from 2 m<sup>3</sup>/s to 15 m<sup>3</sup>/s. The large variations in magma production rates over a timescales of 3-16 Myr could have been caused either by internal dynamics in mantle plume melting process or due to external constraints such as change in the plate velocity, thickness and rheology of the lithosphere, and ridge-plume interactions.

Plate reconstruction studies suggest that the Indian plate had significant variations in its speed during the Cretaceous - Paleocene time (Cande and Stegman 2011, van Hinsbergen *et al.*, 2011, Eagles and Wibisono, 2013, Cande and Patriat, 2015). We observe that onset of rapid movement of the Indian plate under influence of the Reunion Plume at 67 Ma coincides with the decreasing trend in magma production and the lowest magma production occurred during the highest plate velocity (180 mm/yr) at 62 Ma (Figure 2a,b). Subsequent sharp decrease in the plate speed from 180 mm/yr to 100 mm/yr is marked by a steady increase in the magma production rate. A Further phase of slow-down of the Indian plate from 52 Ma onwards as a result of the India-Asia collision is also associated with an increase in

magma production from 50 Ma. These observations are also evident from along axis topographic variations from the predicted topography – lower topography during the periods of low magma production and higher plate speed and *vice-versa* (Figure 2d). The Extremely high velocity attained by the Indian plate is believed to be linked to the exceptionally thin lithosphere beneath India [Kumar et al., 2007]. It is logical to think that a thin lithosphere rapidly responds to the changes in plate velocity and in turn, the rate of magma production rate.

During the phase of high acceleration of the Indian plate, the African plate has experienced significant reduction in its velocity as inferred from the spreading rates of the southern Atlantic Ocean [Cande and Stegman, 2011]. We compared the magma volume flux along the Walvis Ridge [Adam et al., 2007] with the velocity of African plate (Figure 4a,b). It is interesting to note that the peak in magma flux of the Tristan hot spot [Adam et al., 2007] coincides with the minimum velocity period of the African plate (55 Ma). However, in case of the Walvis Ridge the plume pulsations are superimposed on an apparent long-term waning of the plume (Figure 4a). Similar waning signature could be observed in the magma flux along the Reunion plume track (White, 1993, Tiwari et al., 2007). In both cases the effect of plate velocity on magma flux variation may not be clearly distinguishable. Conversely, magma production rate along the NER during the period 80 to 45 Ma did not indicate any waning signature of the Kerguelen plume. We further note that all significant changes in the plate velocity (67 Ma, 62 Ma, 52 Ma) are well reflected in magma flux resulting in long-term variations. The correlations clearly indicate that the lithospheric plate velocity has significant role on controlling the long-period variations in the magma flux assuming there are no significant changes in the magma output from the Kerguelen plume during the emplacement of the NER.

#### ***4.1 Effective elastic thickness, ridge jumps and magma production rates***

Both the NER and Walvis Ridge have variations in effective elastic thickness values, which are highly segmented, because their emplacement process was most probably influenced by the frequent ridge jumps [Watts et al., 2006; Sreejith and Krishna, 2013]. The parameter  $Te$  largely reflects the strength of the lithospheric plate during the emplacement of the volcanic load [Watts, 2001]. Hence, hot spot interaction on a weak lithospheric plate with low  $Te$  value is expected to produce higher volume of magma flux, whereas a strong plate with high  $Te$  resists magma emplacement. However, both features, NER and Walvis Ridge did not show such consistent inverse relationship between  $Te$  and volume flux

(Figures 2a,c and 4a,c). Conversely, in the central part of the NER,  $T_e$  values show a weak positive correlation with the magma production rates.

Observations of bathymetry, gravity and crustal thickness of several migrating ridge – hot spot interactions and numerical simulations suggest that the crustal thickness or volume of magma is inversely dependent on the ridge-hot spot distance and ambient plate velocity [Ito and Lin, 1995, Ito et al., 1997]. The higher plate velocity during the time of emplacement of the central part of the NER (68-62 Ma), may possibly be responsible for continuous changes of spreading center - hot spot geometry, thereby causing the low production rates of the NER. We notice that maximum variations in  $T_e$  associated with the central part of the NER (8°S to 2°N), caused by frequent southward ridge jumps, occurred during the accelerating phase of the Indian plate between 68-65 Ma (Figure 2b,c). The plate velocity slowed down abruptly by about 30% at around 63 Ma followed by a phase of relatively constant velocity for about 10 Myr up to 52 Ma. This phase is largely associated with relatively smaller number of southward ridge jumps [Krishna et al., 2012], less variable  $T_e$  values [Sreejith and Krishna, 2013] and increasing magma production rates (Figure 2a-c). The peak in magma production rate at 57 Ma may probably have coincided with another episode of ridge-hot spot interaction produced by a major southward ridge jump as indicated by progressively increasing  $T_e$  values between 8°S and 18°S. Further, trace element and Sr, Pb and Nd isotope systematics of core and dredged rocks samples from NER clearly indicate mixing of Mid-Ocean Ridge Basalts (MORB) and Ocean Island Basalts (OIB) as a result of the interaction between the Kerguelen hot spot and the spreading center [Weis et al., 1991; Frey and Weis, 1995; Frey et al., 2011]. Thus, it can be inferred that the magma production rates, particularly in the central part of the NER is controlled by spreading rate variations and ridge jumps. The highly variable  $T_e$  values along the ridge could be proxies for the ridge jumps. But  $T_e$  variations may not have directly influenced the magma emplacement rates (Figure 2 a,c). However, along the Reunion track, Tiwari et al., [2007] observed that the increase in  $T_e$  along the hot spot track from north to south is associated with a decreasing magma flux. It should be noted that the systematic decrease in the magma production along the Reunion track could be also explained by the waning of the Reunion plume.

#### **4.2 Short-term periodicity in magma production rate along the NER**

Short-term variations in magma production rate with a periodicity ~5 Myr observed along the NER (Figure 3) may not be associated with the ambient changes in the plate speed [Figures 2a,b]. One possible explanation could be the changes in magma supply produced by tilt in the plume conduit due to

the hot spot motion [Whitehead, 1982; Steinberger, 2000]. However, the motion of the Kerguelen hot spot through time is still not clearly established, although a geodynamic model suggests slow southward motion of  $\sim 5.3$  mm/yr (O'Neill et al., 2003). Alternatively, periodic changes in the magma production can occur due to the formation of solitary waves within the plume conduit [Oslo, 1990; Oslo and Christensen, 1986]. The formation of solitary waves in the plume results in rapid transport of deep mantle materials to the surface [Whitehead and Helfrich, 1988]. Recent high-precision Pb-Hf-Sr-Nd isotopic analyses of the NER basalts indicate heterogeneity in the isotopic compositions both in time and space suggesting multiple sources of origin with intrinsic heterogeneities in the plume [Nobre Silva et al., 2013]. It is possible that intrinsic heterogeneities in the plume related to transport of mantle components to surface may be tied to the propagation of solitary waves in the Kerguelen Plume conduit, but this needs further studies for confirmation. Ito [2001] explained the variations in crustal thickness and magma production along the Reykjanes 'V'-shaped ridges by presence of solitary waves within the Iceland Plume conduit. Similar mechanisms were postulated to explain the short-term variability of Azores [Escartin et al., 2000] and Hawaiian hot spot magma production rates [Van Ark and Lin, 2004; Vidal and Bonneville, 2004]. However, Ballmer et al. [2011] explained the variability in Hawaiian hot spot volcanism with a model, where the plume interacts with alternate thick and thin sections of pre-existing lithosphere created by a small-scale convection. However, this model requires an intraplate setting for the emplacement of the ridge and thus may not be applied directly to the NER.

The changes in the Indian plate speed seem to be the controlling factor for the variations of magma flux rate along the NER. This also indicates that magma production from the Kerguelen plume did not have significant changes, especially at longer timescales, during the emplacement of NER. However, short period oscillations ( $\sim 5$  myr) in the magma production occurred possibly due to the propagation of solitary waves in the plume conduit.

## 5. Conclusions

Magma production rates along the Ninetyeast Ridge (NER) are computed using RMBA derived crustal thickness data. Analysis of spatial variations in the magma production rates along the NER in relation with the Indian plate motion and behavior of the Kerguelen hot spot led to the following conclusions:

- 1) The magma production rates along NER show high variability of  $2-15$  m<sup>3</sup>/s over timescales of 3-16 Myr.

2) Magma production rates, especially the long period changes, possess inverse correlation with the ambient Indian plate velocity during the Late Cretaceous to Early Cenozoic period. The most conspicuous observation is the extremely low production rate along the NER during the unusually rapid motion of the Indian plate (68 - 62 Ma) triggered by the Reunion hot spot and the high magma production along the Walvis Ridge associated with the contemporaneous slowing of the African plate.

3) Long-period magma fluxes (~16 Myr) may be controlled by sharp changes in the Indian plate velocity and frequent ridge jumps, whereas short-period variations (~5 Myr) in the magma production appear to be associated with intrinsic changes in the plume, probably due to the presence of solitary waves in the plume conduit.

### **Acknowledgments**

This work was carried out jointly by SAC-ISRO and CSIR-NIO as a part of the MOP III–Marine Lithospheric Studies program. A.S. Kiran Kumar, P.K. Pal, Manab Chakroborty, and A.S. Rajawat from SAC have supported the collaborative studies. We thank Jon Bull, Fred Frey and an anonymous reviewer for their constructive comments and suggestions. Figures were prepared using GMT software of *Wessel and Smith* [1997]. This is NIO contribution No xxxx.

### **References**

- Adam, C., V. Vidal, and J. Escartín (2007), 80-Myr history of buoyancy and volcanic fluxes along the trails of the Walvis and St. Helena hotspots (South Atlantic), *Earth Planet. Sci. Lett.*, 261, 432–442, doi: 10.1016/j.epsl.2007.07.005.
- Ballmer, M D., G. Ito, Jeroen van Hunen and P.J. Tackley (2011), Spatial and temporal variability in Hawaiian hotspot volcanism induced by small-scale convection, *Nature Geoscience*, doi: 10.1038/NGEO1187
- Cande S. and D.R. Stegman (2011), Indian and African plate driven by the push force of the Reunion plume head, *Nature*, 475, 47-52.
- Cande S.C. and P. Patriat (2015), The anticorrelated velocities of Africa and India in the Late Cretaceous and early Cenozoic, *Geophys. J. Int.*, 200, 227–243.
- Coffin, M., M.S. Pringle, R.A. Duncan, T.P. Gladchenko, M. Storey, R.D Müller, and L.A. Gahagan (2002), Kerguelen hot spot magma output since 130 Ma, *J. Petrol.*, 43, 1121-1139, doi:10.1093/petrology/43.7.1121.
- Curry, J.R. (1994), Sediment volume and mass beneath the Bay of Bengal, *Earth Planet. Sci. Lett.*, 125, 371-383.



- Curry, J. R., F. J. Emmel, D. G. Moore, and W. R. Russell (1982), Structure, tectonics, and geological history of the northeastern Indian Ocean, in *The Ocean Basins and Margins, The Indian Ocean*, vol. 6, edited by A. E. Nairn and F. G. Stheli, pp. 399–450, Plenum, New York.
- Divins, D.L. (2009), NGDC Total Sediment Thickness of the World's Oceans and Marginal Seas. <http://www.ngdc.noaa.gov/mgg/sedthick/sedthick.html>.
- Duncan, R. A. (1991), Age distribution of volcanism along aseismic ridges in the eastern Indian Ocean, *Proc. ODP, Sci. Res.*, 121, 507-517, doi:10.2973/odp.proc.sr.121.164.1991.
- Eagles, G. and A.D. Wibisono (2013), Ridge push, mantle plumes and the speed of the Indian plate, *Geophys. J. Int.*, 194, 670–677.
- Escartin, J., M. Cannat, G. Pouliquen, A. Rabain, and J. Lin (2001), Crustal thickness of V shaped ridges south of the Azores: Interaction of the Mid- Atlantic Ridge (36°–39°N) and the Azores hot spot, *J. Geophys. Res.*, 106, 21,719– 21,735.
- Frey, F. A., and D. Weis (1995), Temporal evolution of the Kerguelen plume: Geochemical evidence from approximately 38 to 82Ma lavas forming the Ninetyeast Ridge, *Contrib. Mineral. Petrol.*, 121, 12–28.
- Frey, F. A., M. Pringle, P. Meleney, S. Huang, and A. Piotrowski (2011), Diverse mantle sources for Ninetyeast Ridge magmatism: Geochemical constraints from basaltic glasses, *Earth Planet. Sci. Lett.*, 303, 215–224, doi:10.1016/j.epsl.2010.12.051.
- Gopala Rao, D., K. S. Krishna, and D. Sar (1997), Crustal evolution and sedimentation history of the Bay of Bengal since the Cretaceous, *J. Geophys. Res.*, 102, 17,747–17,768, doi:10.1029/96JB01339.
- Gordon, R. G., C. DeMets, and J.-Y. Royer (1998), Evidence for long-term diffuse deformation of the lithosphere of the equatorial Indian Ocean, *Nature*, 395, 370– 374, doi:10.1038/26463.
- Grevemeyer, I., E. R. Flueh, C. Reichert, J. Bialas, D. Klaschen, and C. Kopp (2001), Crustal architecture and deep structure of the Ninetyeast Ridge hot spot trail from active-source ocean bottom seismology, *Geophys. J. Int.*, 144, 414–431.
- Ito, G., J. Lin., C.W. and Gable (1997), Interaction of mantle plumes and migrating mid-ocean ridges: Implications for the Galapagos plume-ridge system, *J. Geophys. Res.*, 102, 15403-15417
- Ito, G., J. Lin (1995), Ocean spreading centre-hotspot interactions: Constraints from along-isochron bathymetric and gravity anomalies, *Geology*, 23, 657–660
- Ito, G. T. (2001), Reykjanes ‘‘V’’-shaped ridges originating from a pulsing and dehydrating mantle plume, *Nature*, 411, 681–684.
- Krishna, K.S., D. Gopala Rao, L.V. Subba Raju, A.K. Chaubey, V.S. Shcherbakov, A.I. Pilipenko, and I.V. Radhakrishna Murthy (1999), Paleocene on-axis hot spot volcanism along the Ninetyeast Ridge: An interaction between the Kerguelen hot spot and the Wharton spreading center, *Proc. Indian Acad. Sci. (Earth Planet. Sci.)*, 108, 255-267

- Krishna, K.S., H. Abraham, W.W. Sager, M. Pringle, F.A. Frey, D. Gopala Rao, and O.V. Levchenko (2012), Tectonics of the Ninetyeast Ridge derived from spreading records in adjacent oceanic basins and age constraints of the ridge, *J. Geophys. Res.*, 117, B04101, doi:10.1029/2011JB008805.
- Krishna, K. S., J. M. Bull, and R. A. Scrutton (2001), Evidence for multiphase folding of the central Indian Ocean lithosphere, *Geology*, 29, 715–718.
- Krishna, K. S., J. M. Bull, and R. A. Scrutton (2009), Early (pre-8 Ma) fault activity and temporal strain accumulation in the central Indian Ocean, *Geology*, 37, 227–230.
- Kumar P., X. Yuan X., M. Ravi Kumar, R. Kind, X. Li and R. K. Chadda (2007), The rapid drift of the Indian tectonic plate, *Nature*, 449, 894-897.
- Levchenko, O. V., V. Y. Milanovskiy, and A. A. Popov (1993), A sediment thickness map and the tectonics of the distal Bengal Fan, *Oceanology*, 33(2), 232–238.
- Mjelde, R. P. Wessel and R.D. Müller (2010), Global pulsations of intraplate magmatism through the Cenozoic, *Lithosphere*, 2, 361-376.
- Müller, R. D., M. Sdrolias, C. Gaina, and W. R. Roest (2008), Age, spreading rates, and spreading asymmetry of the world's ocean crust, *Geochem. Geophys. Geosyst.*, 9, Q04006, doi:10.1029/2007GC001743.
- Nobre Silva, I. G., D. Weis, D., J.S., Scoates and J. Barling (2013), The Ninetyeast Ridge and its Relation to the Kerguelen, Amsterdam and St. Paul Hotspots in the Indian Ocean, *J. Petrol.*, 1-34.
- Olson, P. (1990), Hot spots, swells and mantle plumes, in *Magma Transport and Storage*, edited by M. Ryan, pp. 33–51, John Wiley, Hoboken, N. J.
- Olson, P., and U. Christensen (1986), Solitary wave propagation in a fluid conduit within a viscous matrix, *J. Geophys. Res.*, 91, 6367– 6374.
- O'Neill, C., D. Müller, and B. Steinberger (2003), Geodynamic implications of moving Indian Ocean hot spots, *Earth Planet. Sci. Lett.*, 215, 151-168.
- Pringle, M.S., F.A. Frey, and E.M. Mervine (2008), A simple linear age progression for the Ninetyeast Ridge, Indian Ocean: New constraints on Indian plate motion and hot spot dynamics, *EOS, Trans. AGU*, 89 (53) Fall Mtg. Suppl., abstract T54B-03.
- Royer, J.-Y., J. W. Peirce, and J. K. Weissel (1991), Tectonic constraints on the hotspot formation of Ninetyeast Ridge, *Proc. Ocean Drill. Program Part B Sci. Results*, 121, 763–776.
- Royer, J.-Y., and R.G. Gordon (1997), The motion and boundary between the Capricorn and Australian plates: *Science*, 277, 1268–1274, doi: 10.1126/science.277.5330.1268.
- Sager, W.W., C.F. Paul, K.S. Krishna, M. Pringle, A.E. Eisin, F.A. Frey, D. Gopala Rao, and O. Levchenko (2010), Large fault fabric of the Ninetyeast Ridge implies near spreading ridge formation, *Geophys. Res. Lett.*, 37, L17304, doi:10.1029/ 2010GL044347.

- Sager, W. W., J. M. Bull, and K. S. Krishna (2013), Active faulting on the Ninetyeast Ridge and its relation to deformation of the Indo-Australian Plate, *J. Geophys. Res. Solid Earth*, 118, 4648–4668, doi:10.1002/jgrb.50319.
- Sandwell, D.T., and W.H.F. Smith (2009), Global marine gravity from retracked Geosat and ERS-1 altimetry: Ridge segmentation versus spreading rate, *J. Geophys. Res.*, 114, B01411, doi:10.1029/2008JB006008.
- Smith, W.H.F., and D.T. Sandwell (1997), Global seafloor topography from Satellite altimetry and ship depth soundings, *Science*, 277, 1956–1962.
- Sreejith, K.M., and K.S. Krishna (2013), Spatial variations in isostatic compensation mechanisms of the Ninetyeast Ridge and their tectonic significance, *J. Geophys. Res.*, 118, 1–20, doi:10.1002/jgrb.50383, 2013.
- Steinberger, B. (2000), Plumes in a convecting mantle: Models and observations for individual hotspots, *J. Geophys. Res.*, 105, 11,127–11,152.
- Tiwari, V.M., I. Grevemeyer, B. Singh, J. Phipps Morgan (2007), Variation of effective elastic thickness and melt production along the Deccan–Reunion hotspot track, *Earth Planet. Sci. Lett.*, 264, 9–21.
- Van Ark, E., and J. Lin (2004), Time variation in igneous volume flux of the Hawaii-Emperor hot spot seamount chain, *J. Geophys. Res.*, 109, B11401, doi:10.1029/2003JB002949
- van Hinsbergen, D.J.J., B. Steinberger, P.V. Doubrovine and R. Gassmüller, R (2011), Acceleration and deceleration of India-Asia convergence since the Cretaceous: roles of mantle plumes and continental collision, *J. Geophys. Res.*, 116, B06101, doi:10.1029/2010JB008051.
- Vidal, V., and A. Bonneville (2004), Variations of the Hawaiian hot spot activity revealed by variations in the magma production rate, *J. Geophys. Res.*, 109, B03104, doi:10.1029/2003JB002559.
- Watts, A.B. (2001), *Isostasy and flexure of the lithosphere*, Cambridge University Press, UK.
- Watts, A. B., D. T. Sandwell, W. H. F. Smith, and P. Wessel (2006), Global gravity, bathymetry, and the distribution of submarine volcanism through space and time, *J. Geophys. Res.*, 111, B08408, doi:10.1029/2005JB004083.
- Weis, D., F. A. Frey, A. Saunders, and I. Gibson (1991), Leg 121 Scientific Shipboard Party, Ninetyeast Ridge (Indian Ocean): A 5000 km record of a Dupal mantle plume, *Geology*, 19, 99–102.
- White, R. (1993), Melt production rates in mantle plumes, *Philos. Trans. R. Soc. London, Ser. A*, 342, 137–153.
- Whitehead, J. (1982), Instabilities of fluid conduits in a flowing Earth—Are plates lubricated by the asthenosphere?, *Geophys. J. R. Astron. Soc.*, 70, 415–433.
- Whitehead, J., and K. Helfrich (1988), Wave transport of deep mantle material, *Nature*, 338, 59–61.

## **Figure Captions:**

**Figure 1:** Seafloor topography of the NER from ETOPO-1. Magnetic lineations (thin line), fossil spreading centers (thick dashed lines) and fracture zones (dashed line) of the region adjacent to the NER [Krishna *et al.*, 2012] are placed over the map. DSDP and ODP sites (solid circles) are shown with geochronology dates (Ma) in brackets. New age dates are shown to drill sites except DSDP site 217 [Pringle *et al.*, 2008]. SUM = Sumatra

**Figure 2:** (a) Variations of magma production rates as a function of interpolated age of volcanism along the NER. (b) Variations in the Indian plate motion as indicated by changes in spreading rates along a synthetic flow line across the India-Antarctica Ridge [Cande and Stegman, 2011]. (c) Plot showing  $T_e$  values along the NER from 28°S to 8°N derived from 2-D and 3-D flexural modeling [Sreejith and Krishna, 2013]. The lower and upper bounds of  $T_e$  estimates using 2D and 3D methods are indicated by gray shading and error bars. (d) Bathymetry (Black line), predicted water depths (dashed line), DSDP and ODP drill locations (arrows) and gravity (Gray line) on a longitudinal transect along the NER.

**Figure 3:** Power spectral density of the magma production rates as shown in Figure 2a. The spectra were computed using Fast Fourier Transform with a symmetrical Hanning window. The periods corresponding to the peaks in spectrum are indicated.

**Figure 4:** (a) Variations of magma production rates as a function of interpolated age of volcanism along the Walvis Ridge [Adam *et al.*, 2007]. (b) Variations in the Atlantic plate motion [Cande and Stegman, 2011]. Magma flux >65 Ma are not plotted as their origin is suspected to be non-plume in nature. (c)  $T_e$  values [Watts *et al.*, 2006] projected along the axis of the Walvis Ridge

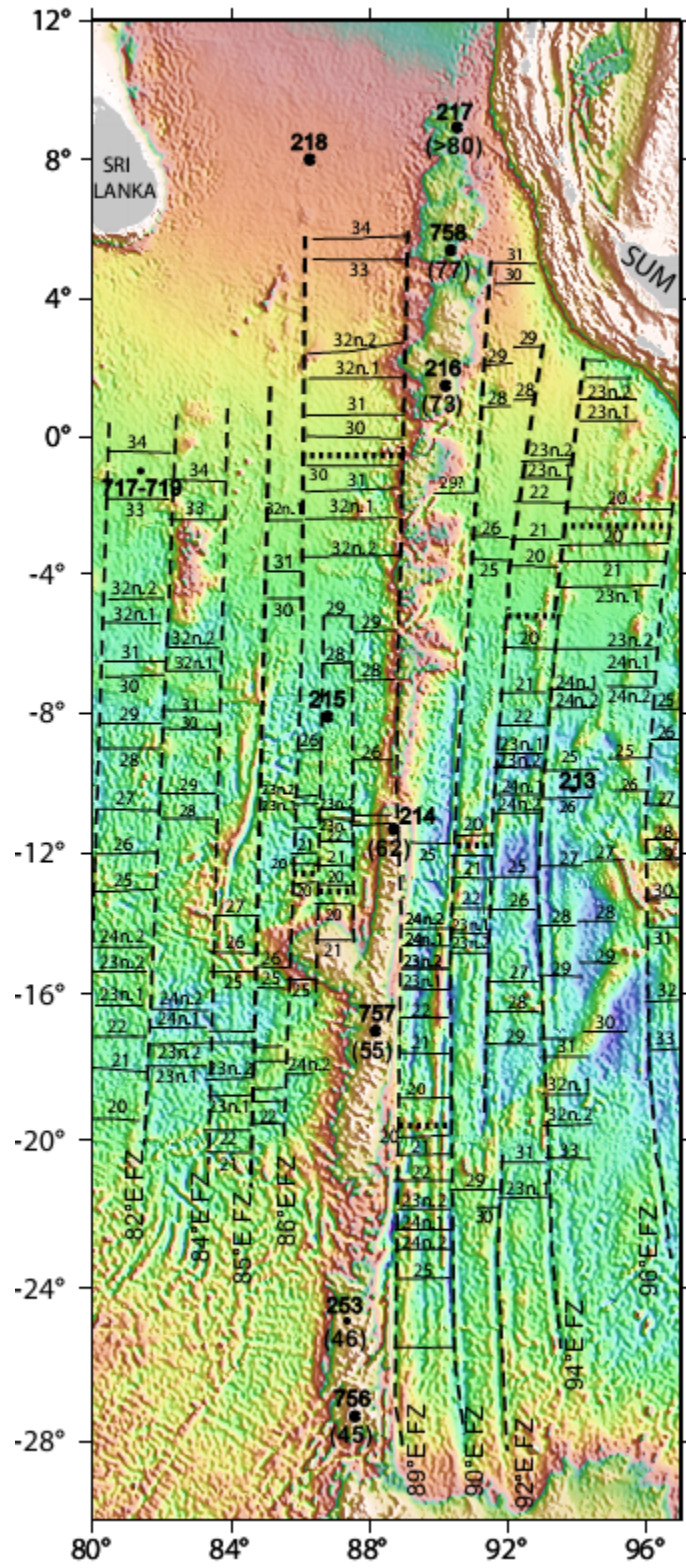


Figure 1

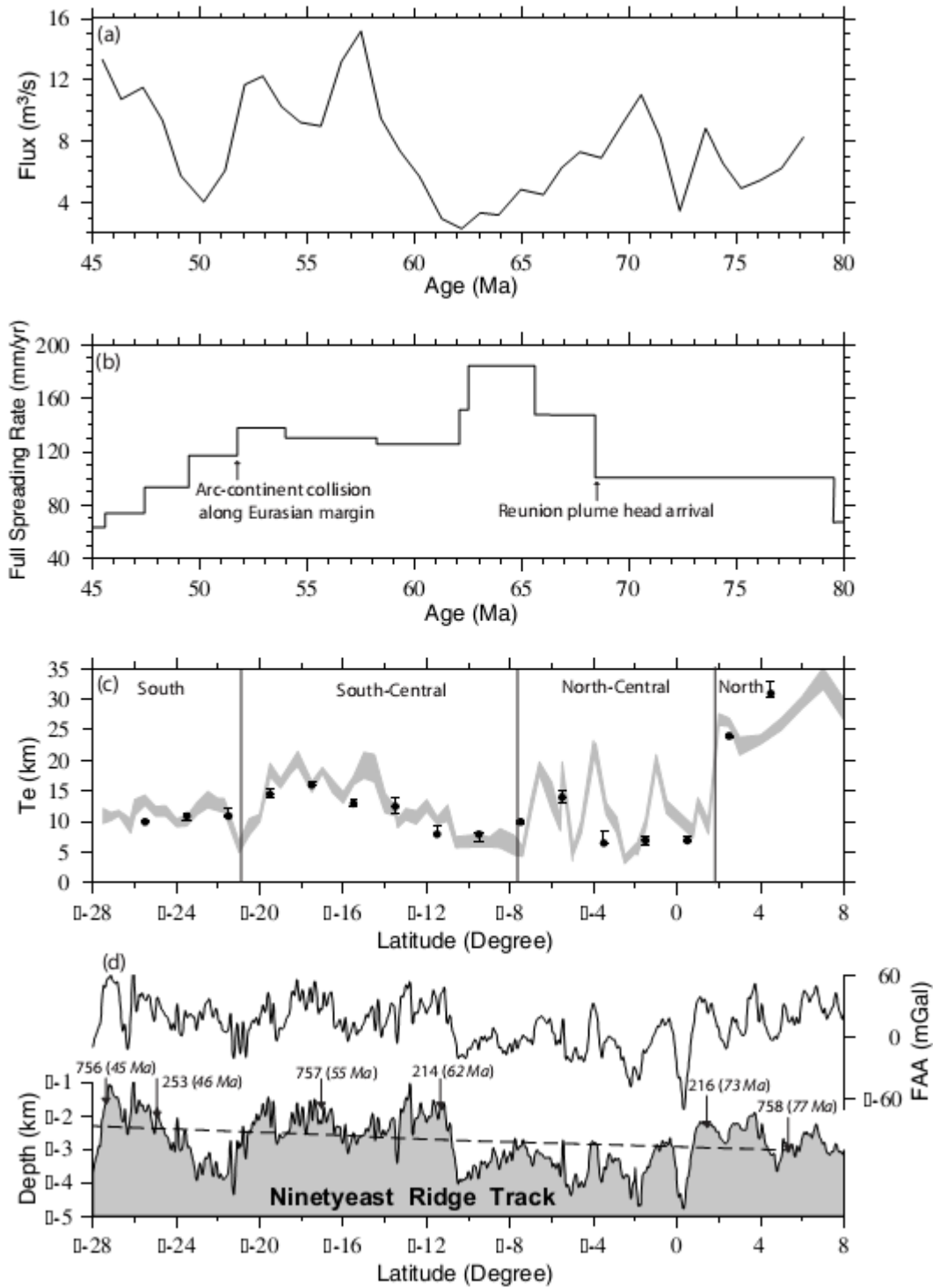
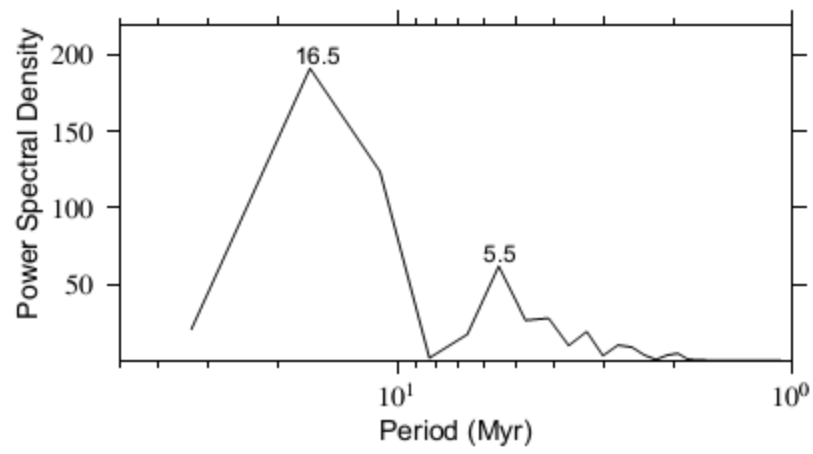


Figure 2:



**Figure 3**

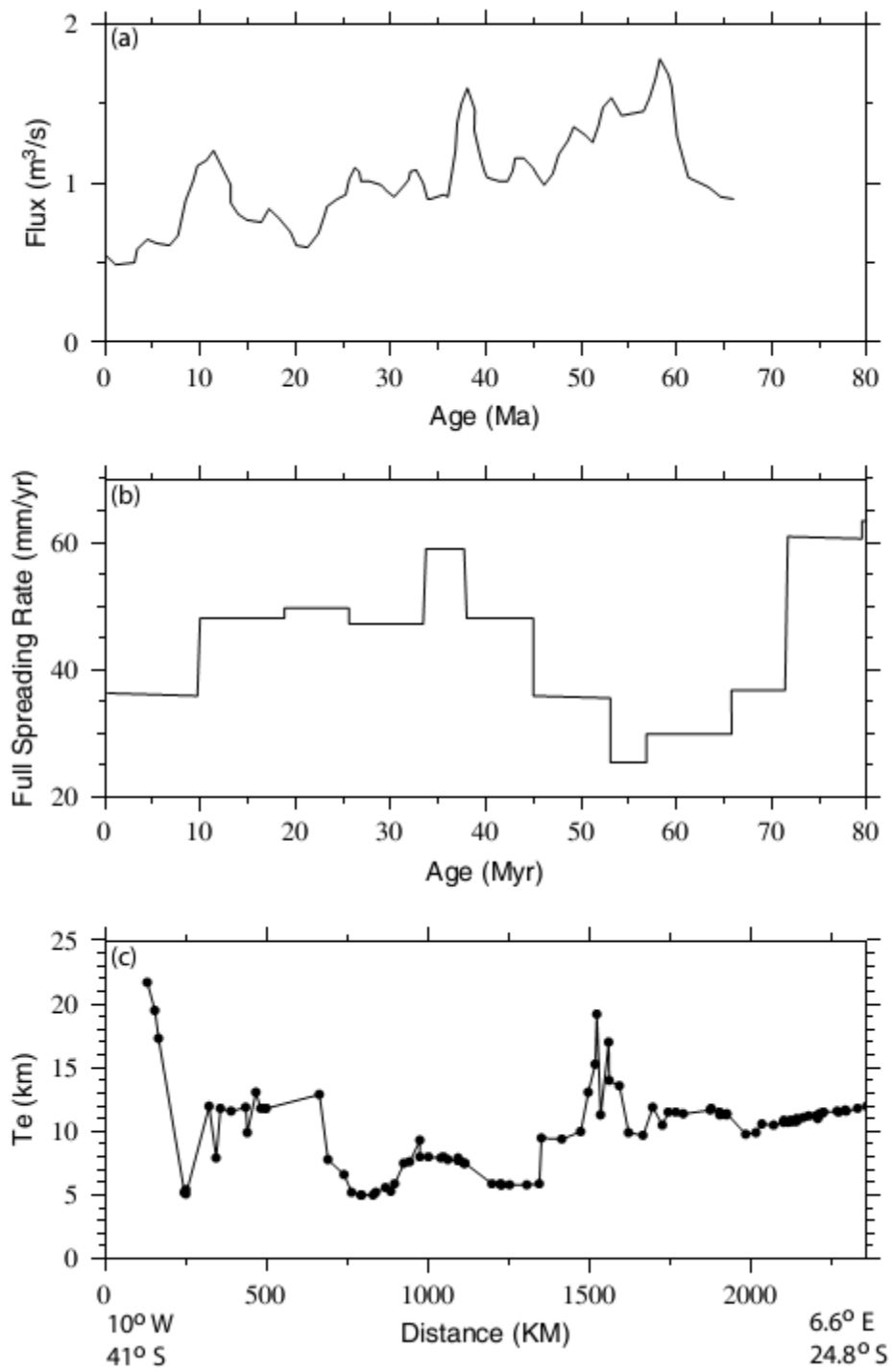


Figure 4